Journal of Water Process Engineering 60 (2024) 105101

Contents lists available at ScienceDirect

Journal of Water Process Engineering

journal homepage: www.elsevier.com/locate/jwpe

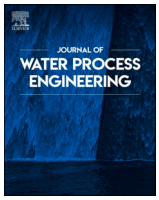

Recovery of microbial biomass and purification performance after scraping of full-scale slow sand filters

Shreya Ajith Trikannad [a,*], Valentina Attiani [b,1], Paul W.J.J. van der Wielen [b,c], Hauke Smidt [b], Jan Peter van der Hoek [a,d], Doris van Halem [a]

[a] Water Management Department, Delft University of Technology, Building 23 Stevinweg 1, 2628 Delft, the Netherlands
[b] Laboratory of Microbiology, Wageningen University & Research, P.O. Box 8033, 6700 EH Wageningen, the Netherlands
[c] KWR Watercycle Research Institute, P.O. Box 1072, 3430 BB Nieuwegein, the Netherlands
[d] Waternet, Korte Ouderkerkerdijk 7, 1096 AC Amsterdam, the Netherlands

ARTICLE INFO

Editor: Rong Chen

Keywords:
Slow sand filters
Schmutzdecke
Scraping
Ripening period
Dissolved organic carbon
Ammonium

ABSTRACT

Slow sand filters (SSFs) are widely used in drinking water production to improve microbial safety and biological stability of water. Full-scale SSFs are maintained by scraping the biomass-rich top layers of sand. The period of downtime required for filter recovery after scraping is a major challenge due to limited knowledge of the re-stabilisation of purification processes. This study examined the recovery of microbial biomass, and removal of dissolved organic carbon (DOC) and ammonium (NH_4^+) in water phase and/or on sand along the depth of a scraped full-scale SSF. Scraping reduced microbial biomass on sand in the top layers, while the main prokaryotic taxa remained unaltered. Cellular ATP (cATP) and intact cell counts (ICC) in water sampled from the top layers increased, indicating a temporary disruption in functionality for 37 days. However, stable concentrations of cATP and ICC and similar microbial community composition in the effluent after scraping revealed that deeper layer biofilms offset any scraping effect. Consistent DOC and NH_4^+ removal after scraping showed that deeper layers effectively performed the role of the top layer. These findings highlight the resilience and robustness of microbial communities in mature full-scale SSFs and their contribution to water treatment efficiency after disturbances caused by scraping.

1. Introduction

Water utilities aim to produce microbiologically safe and biologically stable drinking water to prevent microbial regrowth during distribution [1]. Slow sand filters (SSFs) are a third or final polishing step in drinking water production to remove turbidity, pathogens, dissolved organic carbon (DOC) and ammonium (NH_4^+) [2,3]. SSFs are energy-efficient, require no additional chemicals and produce minimal waste, making them a sustainable choice for drinking water production in both developed and developing countries [4].

SSFs purify water by interdependent biological and physical-chemical processes, and the indigenous microbial community that inhabit the sand bed play a crucial role [5–7]. The *Schmutzdecke*, a highly active, biomass-rich layer top layer forms a primary barrier for several contaminants. Excessive biomass accumulation over time restricts hydraulic flow in the filter, thus, the top few layers are periodically scraped [8]. In full-scale SSFs, *Schmutzdecke* scraping often leads to a downtime or ripening period until filter activity recovers and effluent quality meets regulatory standards. This period can be lengthy or short, depending on filter age and maturity of microbial communities on sand [9].

Former investigations performed in lab and pilot-scale SSFs showed that scraping invariably reduced *E. coli* and coliforms removal [10]. A full-scale SSF study found minimal effect of *Schmutzdecke* removal on total organic carbon (TOC) and bacterial indicator removal [9]. A lab-scale investigation showed that scraping significantly changed microbial community composition in the top layer but did not compromise turbidity and total coliform removal [11]. These inconsistencies may result from differences in filter maturity in young lab/pilot-scale filters which might not accurately represent well-established full-scale SSFs. Despite some insights on the impact of scraping, knowledge on re-stabilisation of DOC and NH_4^+ removal processes after scraping, from a biological stability perspective is limited. Moreover, the recovery of microbial communities during ripening of mature full-scale SSFs has not been thoroughly explored.

* Corresponding author.
E-mail address: S.A.Trikannad@tudelft.nl (S.A. Trikannad).
[1] Shared first authorship.

https://doi.org/10.1016/j.jwpe.2024.105101
Received 22 January 2024; Received in revised form 22 February 2024; Accepted 29 February 2024
Available online 8 March 2024
2214-7144/© 2024 The Author(s). Published by Elsevier Ltd. This is an open access article under the CC BY license (http://creativecommons.org/licenses/by/4.0/).

DOC in water primarily consists of refractory (i.e. poorly biodegradable) compounds, biodegradable dissolved organic carbon (BDOC) and easily assimilable organic carbon (AOC) [12,13]. BDOC and AOC fractions in drinking water can stimulate bacterial regrowth during distribution [14]. Slowly biodegradable organic carbon fractions such as biopolymers negatively affect the biological stability of drinking water [15]. Due to the importance of both slowly and easily biodegradable organic carbon fractions, DOC is widely measured amongst other biostability parameters such as AOC, BDOC, biomass and Biofilm Formation Rate (BFR) [13,16,17]. Typically in SSFs, DOC is removed by a combination of biological (bacterial respiration and biomass assimilation) and physical-chemical processes [18–20]. NH_4^+ is removed by assimilation and by nitrifying microorganisms that oxidize NH_4^+ to NO_2^- and subsequently NO_3^- [21] or directly from NH_4^+ to NO_3^- [22]. Since both DOC and NH_4^+ removal depend on microbial activity, it is important to examine how scraping influences the recovery of removal processes.

Our knowledge of filter ripening is often limited due to the inability of current routine analyses to describe the recovery of microbial communities and purification processes in real or near-real time. After scraping, the effluent of full-scale SSFs is typically monitored for heterotrophic plate counts (HPC) and the absence of pathogen indicator organisms like *Escherichia coli*, total coliforms, enterococci and *Clostridium*. When SSFs are at the end of the treatment train and receive a low microbial load, pathogen indicators might not always be detected in the influent [3]. Earlier studies have emphasized the ability of rapid methods such as flow cytometry (FCM) for assessing prokaryote cell numbers and adenosine triphosphate (ATP) for detecting changes in cell numbers and active biomass in water treatment [9,23–26]. Chan et al. showed that abnormal changes in bacterial profiles of SSF effluent measured by FCM could indicate disturbances in the treatment process [9].

The objective of this study was to evaluate the recovery of microbial biomass and communities and the removal of DOC and NH_4^+ after scraping in a mature full-scale SSF. To this end, a scraped full-scale SSF was compared with an unscraped full-scale SSF and monitored throughout the ripening process. To the best of our knowledge, this is the first study examining depth profiles of operating full-scale SSFs for changes in ATP, cell counts, 16S ribosomal RNA (rRNA) gene copies, microbial community composition in water and on filter sand, and DOC and NH_4^+ in the water phase.

2. Materials and methods

2.1. Description of SSFs

Two full-scale SSFs at a drinking water treatment plant in Scheveningen (The Netherlands) of drinking water company Dunea were investigated in this study. The plant receives raw water from the river Meuse and is further treated by managed aquifer recharge in the dunes, pellet softening, aeration, rapid sand filtration with powdered activated carbon dosing and slow sand filtration before distribution. Both SSFs, located in the same production line, were built in 1955 and have been producing drinking water for the last 28 years without sand replacement. The operational parameters and influent water characteristics of both filters are shown in Table 1. The SSFs become clogged every few years due to excessive biofilm accumulation in the *Schmutzdecke* layer and, consequently, filters are scraped every few years to remove the clogged top layer of the filter. One of the filters in our study (Scraped filter) was scraped after 5.3 years of continuous operation by removing the top 10 cm of the sand bed, while the second filter (Control filter), which was last scraped 4.6 years ago, was used as a control.

2.2. Sand sampling

On day 0, the supernatant water was lowered below the filter bed to allow for sand scraping in the scraped filter. Just before scraping, a sand core was sampled from the scraped filter by using a sterile aluminium sediment sampler. The sand core was divided into different sections (0–2 cm, 0–5 cm, 10–15 cm, and 20–25 cm) and collected into 15 mL sterile falcon tubes. The selected filter depths represent the *Schmutzdecke* (0–2 cm), top (0–5 cm) and middle (10–15 and 20–25 cm) layers of the sand bed. The sand sampling depth was restricted to 25 cm to prevent sampling disturbances in the deep sand bed, which could negatively affect the quality of the produced drinking water. Hence, the sand sampling is not representative of the overall filter bed performance but gives a good indication of what happens in the first 25 cm of the sand bed.

After restarting the filter, only the top 0–2 cm sand layer was sampled using a telescopic sampler from scraped and control SSFs on the same day and around the same time. Sand from the surface layer was sampled on days 1, 8, 15, 28, 36, 52, 80, 100, and 120 after scraping, to better understand biomass recovery during operation (Fig. 1A). The sand collected on days 0, 8, 15, 28 and 52 was used for microbial community composition analysis. Two replicate samples were collected from the sampling point shown in Fig. S1 and transported to the laboratory in Styrofoam boxes containing icepacks. The first replicate samples were stored at −20 °C on the same day for DNA extraction. Other replicate samples were stored at 4 °C and used for cellular ATP (cATP) and cell count measurements on the same day.

Table 1
Operational parameters, influent and effluent characteristics of scraped and control full-scale SSFs. Historical data refer to average and standard deviation of the biweekly concentrations between June 2020 and August 2022.

	Unit	Scraped filter	Control filter
Filter bed height	m	0.95	0.8
Height of supernatant	m	1	1
Filter area	m^2	2383	2359
Filtration rate	m/h	0.4	0.4
Grain size	mm	0.3–0.6	0.3–0.6
Age of media	years	28	28
Time since last scraping	years	5.3	4.6

Historical data	Unit	Influent	Effluent	
Temperature	°C	14.2 ± 2.68	14.5 ± 2.68	14.3 ± 2.68
ATP	pg/mL	6.24 ± 0.08	1.5 ± 0.08	1.41 ± 0.07
ICC	cells/mL	2.66 × 105 ± 0.03	1.66×10^5 ± 0.03	1.70×10^5 ± 0.03
TCC	cells/mL	4.70 × 105 ± 0.04	2.70×10^5 ± 0.04	2.59×10^5 ± 0.03
AOC	µg C/L	5.45 ± 0.04	3.7 ± 0.04	3.8 ± 0.05
DOC	mg C/L	3.65 ± 0.02	2.65 ± 0.02	2.7 ± 0.03
NO_3^-	mg N/L	0.98 ± 0.01	1.20 ± 0.01	1.25 ± 0.02
NH_4^+	mg N/L	0.009	0.006	0.006
NO_2^-	mg N/L	0.001	0.001	0.001
Turbidity	NTU	2.11 ± 0.01	1.36 ± 0.01	1.39 ± 0.01
Coliforms	CFU/L	0 ± 2	0	0
Escherichia coli	CFU/L	0 ± 1	0	0
Sulfite-reducing clostridia	CFU/L	0 ± 1	0	0

CFU - colony forming unit.

2.3. Water sampling

The water used to measure the chemical and microbial biomass parameters was sampled from both filters at influent, effluent and at four different depths (15, 25, 35 and 55 cm) (Fig. 1B). The water was collected using sampling ports provided on the filter wall with 30 cm long pipes penetrating the sand bed. The first water sampling over the height was conducted one day before scraping, (i.e., day −1) as the filter had to be drained completely on day 0 for the scraping. Thereafter, water was sampled on days 8, 15, 28 and 37 after scraping (Fig. 1A).

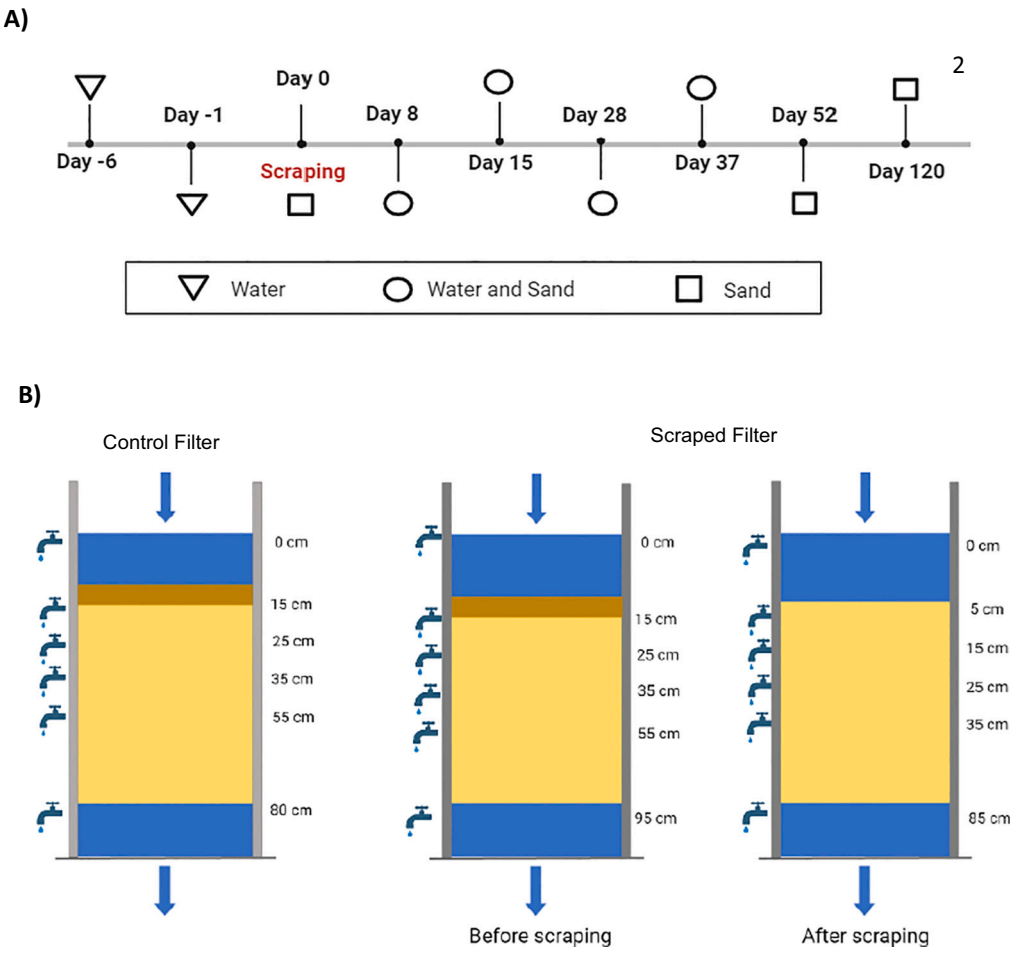

Fig. 1. (A) Overview of sand and water sampling in scraped and control SSFs, (B) Schematic diagram of the SSFs and sampling points.

The water used for the microbial community analysis was sampled from the influent and effluent points of the scraped filter. The water was collected in duplicates of 1 L using sterile plastic bottles (Identipack, the Netherlands) 6 days before and 15 days after scraping. The samples were transported to the laboratory in Styrofoam boxes containing icepacks and were filtered with 0.2 µm filter (Isopore TM PC membrane, 47 mm hydrophilic, Merck, Millipore) within 24 h from sampling to collect microorganisms. The filters were stored at −20 °C until DNA extraction.

2.4. Water analyses

Microbial cATP, which is indicative of the active biomass, was measured using Quench-Gone aqueous test kit and a LB9509 luminometer (Aqua Tools, France) as per the manufacturer's protocol. Flow-cytometry analysis was carried out with BD AccuriC6® FCM (BD Biosciences, Belgium) at Het Waterlaboratorium (Haarlem, the Netherlands). Sample volumes of 260 µL were drawn at a flow rate of 200–400 mL/min and mixed with fluorescent stain (SYBR®Green, propidium iodide). After incubation (10 min, 37 °C), samples were analysed (FL1 channel at 525 nm, FL3 channel at 721 nm) using fixed gates to separate cells and background signals and additionally to distinguish between so-called high nucleic acid (HNA) and low nucleic acid (LNA) content cells cATP and ICC measured in water will be referred to as $cATP_w$ and ICC_w.

DOC (Limit of Detection [LOD] = 0.1 mg/L) was measured with a Shimadzu TOC-$V_{CPH/CPN}$ analyser with a standard deviation of 0.1 mg/L immediately or within one day after sampling. 30 mL of sample was filtered through 0.45 µm filters (SPARTAN™, Whatman, Germany) that had been flushed twice with demineralized water. Samples for NH_4^+ (LOD = 0.01 mg/L) and NO_3^- (LOD = 0.1 mg/L) were immediately filtered through a 0.22 µm nanopore filter and measured within 12 h using Ion Chromatography (Dionex ICS-2100, Thermo, USA) equipped with an AS17-Column with a detection limit of 0.01 mg/L.

2.5. Sand analyses

cATP was measured on filter sand with 1 g of wet media sample, following the Deposit and Surface Analysis test kit method from LuminUltra Technologies [27]. Measurements were read using a luminometer. ICC measurement was conducted at Het Waterlaboratorium (Haarlem, the Netherlands). cATP and ICC measured on sand will be referred to as $cATP_s$ and ICC_s.

2.6. Molecular analysis

2.6.1. DNA isolation and library preparation

The DNA from water samples was extracted using the DNeasy PowerBiofilm Kit (QIAGEN, Hilden, Germany) according to the manufacturer's instruction except for the first step for which the thawed filters were placed directly into the PowerBeads tubes. The DNA from sand samples was isolated with the Powersoil Pro kit (QIAGEN, Hilden, Germany) using a range of 0.5–1 g of sand as starting material. The amount of sand used was noted for future reference and normalization. A negative control consisting of one empty PowerBead Pro Tube was included during DNA extraction for quality control. For both water and sand samples, the bead beating step was performed using the FastPrep-24 5G bead beating grinder and lysis system (MP Biomedicals, Irvine, United States), and by applying one cycle at 4.0 m/s for 45 s. After DNA extraction, DNA concentrations were measured fluorometrically (Qubit

dsDNA BR assay, Invitrogen) and the DNA was stored at −20 °C.

The hypervariable region V4 (~290 bp) of the bacterial and archaeal 16S rRNA gene was amplified from the extracted DNA with a PCR reaction prepared with 10 μL of 5× Phusion Green HF Buffer (Thermo Scientific, US), 1 μL of 10 μM barcoded primers 515F-n (5′-GTGYCAGCMGCCGCGGTAA-3′) and 806R-n (5′-GGACTACNVGGGTWTCTAAT-3′) [28,29], 1 μL of 10 mM dNTPs mix (Promega Corporation, US), 0.5 μL of 2 U/μL Phusion Green Hot Start II HF DNA polymerase (Thermo Scientific, US), the DNA template (final concentration of ~20 ng/μL DNA) and Nuclease-free water to reach a final volume of 50 μL. Positive controls, non-template controls (only PCR mix) and negative controls (PCR mix and Nuclease-free water instead of the template DNA) were included in the PCR analyses for quality check. The amplification program included an initial step of 98 °C for 30 s, then 28 cycles at 98 °C for 10 s, followed by an annealing step at 50 °C for 10 s and elongation step at 72 °C for 10 s, and a final extension at 72 °C for 7 min. The presence and length of PCR products were verified by gel electrophoresis. Subsequently, PCR products were purified using CleanPCR magnetic beads kit (CleanNA, Netherlands) according to the manufacturer's protocol. Purified products were quantified fluorometrically (Qubit dsDNA BR assay, Invitrogen) and quantified using the Qubit dsDNA BR Assay kit (Invitrogen by Thermo Fisher Scientific, Eugene, OR, USA). The clean samples were pooled in equimolar amounts into libraries, including negative and positive controls. After pooling, the mixed libraries were purified and concentrated again using CleanPCR magnetic beads to a concentration final volume of 40 μL. The final purified PCR products including those amplified from SSFs samples, positive and negative controls were sequenced on an Illumina Novaseq 6000 platform at Novogene (Cambridge, United Kingdom). Raw 16S rRNA gene sequences with barcode and primer removed and supporting metadata were deposited in the European Nucleotide Archive (http://www.ebi.ac.uk/ena) under accession number PRJEB72542.

2.6.2. qPCR

Quantitative PCR (qPCR) was used to measure the copy numbers of the total bacterial 16S rRNA genes of the DNA from sand and water samples. The DNA concentrations were adjusted to 1 ng/μL by diluting original extracts in DNase/RNase free water before use as the template in qPCR. The qPCR mix was composed of iQTM SYBR Green Supermix (Bio-Rad Laboratories, USA), universal primers targeting the 16S rRNA gene (1369F 5′-CGGTGAATACGTTCYCGG-3′ and 1492R 5′-GGWTACCTTGTTACGACTT-3′; 123 bp), 1 μL of DNA template and sterile nuclease-free water in a total volume of 10 μL. Each sample was assayed in technical triplicates by using a C1000 Thermal Cycler (CFX384 Real-Time system, Bio-Rad Laboratories, USA) with the following protocol: 95 °C for 10 min followed by 40 cycles of 95 °C for 15 s, 60 °C for 30 s and 72 °C for 15 s each; then one cycle of 95 °C for 1 min; and a stepwise increase of temperature from 60 °C to 95 °C (at 0.5 °C per 5 s) to obtain melt curve data. The qPCR data was analysed using CFX Maestro 2.3 (Bio-Rad) and Microsoft Excel (version 2021).

2.6.3. Bioinformatic analysis of 16S rRNA gene sequence data

NG-Tax 2.0 was used for processing of 16S rRNA gene sequence data with default settings [30,31]. Subsequently, amplicon sequence variants (ASVs) were identified on a per sample basis. Taxonomic assignment of ASVs was performed referring to the SILVA 138.1 database [32]. All bioinformatic analyses were conducted in R (version 4.2.1) using the packages *phyloseq* (v 1.42.0) [33], *microViz* (v 0.11.0) [34], *ggplot2* (v 3.4.3), *ggsignif* (v 0.6.4) [35], *dplyr* (v 1.1.3), *speedyseq* (v 0.2.0) [36], *RColorBrewer* (v 1.1-3) [37] and *vegan* (v 2.6-4) [38].

2.7. Statistical analysis

Statistical analysis was performed on all quantitative data (cATP, cell counts, DOC, NH_4^+ and 16S rRNA gene copies) using one-way ANOVA, followed by the Bonferroni post-hoc correction.

3. Results

3.1. Microbial biomass and activity

Total bacterial 16S rRNA gene copies (via qPCR), $cATP_s$ and ICC_s were used as complementary indicators to measure the total biomass in sand and water. While qPCR accounts for both dead and viable cells, $cATP_s$ indicates active biomass and ICC_s cells with an intact membrane.

Before scraping, the top 0–2 cm sand layer in the scraped filter showed the highest 16S rRNA gene copy numbers compared to its deeper sections (Fig. 2A). During scraping, the top 10 cm of the sand bed

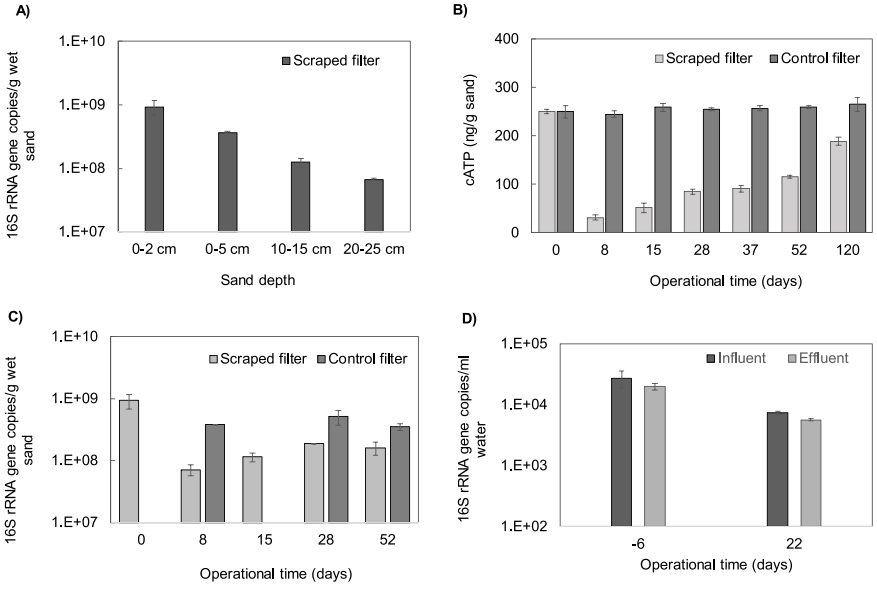

Fig. 2. Microbial biomass in sand samples. (A) Total bacterial 16S rRNA gene copies in sand at different depths of scraped filter before scraping, (B) $cATP_s$ in the top sand layer (0–2 cm) of control and scraped filter during operation, (C) Total bacterial 16S rRNA gene copies in the top layer (0–2 cm) of control and scraped filter, (D) Total bacterial 16S rRNA gene copies in water influent and effluent of the scraped filter 6 days before and 15 days after scraping. The measurements were carried out in triplicates; error bars represent standard deviation.

was removed from the filter. Eight days after scarping, the bacterial biomass on the top layer of sand was significantly lower as compared to the filter before scraping and the control filter (Figs. 2B and C, S2) (qPCR, $cATP_s$ and ICC_s $p = 0.004$). The 16S rRNA gene copies and $cATP_s$ in the top layer sand (0–2 cm) decreased by 13 and 6 times, respectively. However, the biomass concentrations in the top layer of scraped filter gradually increased over time as filtration progressed, approaching the level prior to scraping. In comparison, the top layer of the control filter maintained stable biomass throughout the experimental period (qPCR, $cATP_s$ and ICC_s $p = 0.09$) (Fig. 2B and C).

Microbial biomass in water along the filter height was assessed using $cATP_w$ and ICC_w (Fig. 3). One day before scraping, both filters showed a

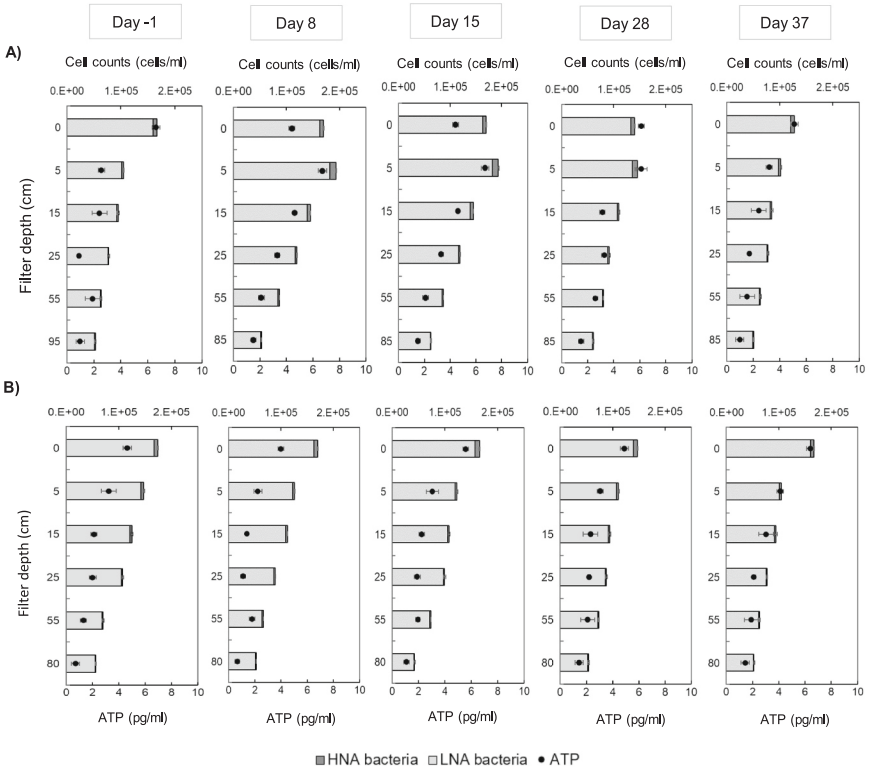

Fig. 3. Depth profiles of $cATP_w$, HNA and LNA cells within ICC_w in water in scraped (A) and control (B) filters during filter operation. Measurements were carried out in triplicates; error bars represent standard deviation.

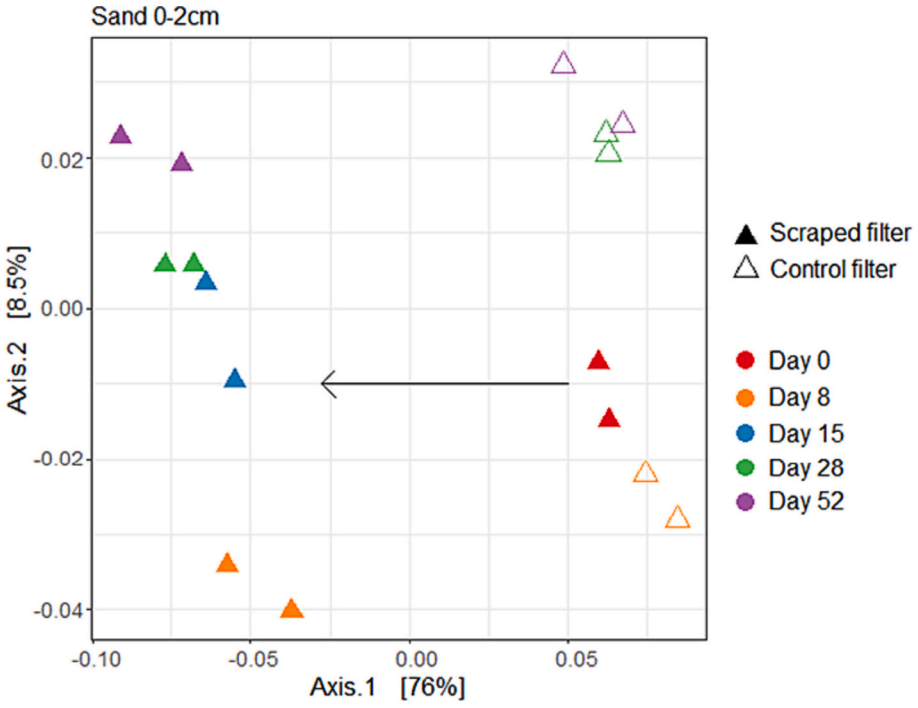

Fig. 4. PCoA plot showing the temporal variation in Beta Diversity (Weighted UniFrac) analysis of sand samples (0–2 cm) collected from scraped and unscraped filters.

decrease in $cATP_w$ and ICC_w with depth. After scraping, $cATP_w$ and ICC_w were significantly higher within the top 25 cm of the scraped filter on days 8 and 15, in contrast to the control filter ($p = 0.0002$). At 5 cm depth, the concentrations of HNA and LNA cells within the ICC and cATP increased significantly ($p = 0.006$) by 68 %, 14 % and 50 %, respectively compared to the influent (0 cm). Despite this breakthrough of biomass in the top layers, the effluent ATP, HNA and LNA cell concentrations remained stable throughout (Fig. S3). From day 28, the disturbed depth profile of the biomass parameters in the scraped filter began shifting towards the concentrations obtained before scraping and in the control SSF, suggesting complete restoration by day 37. In the scraped filter, bacterial biomass in the effluent water, measured with qPCR, was significantly lower than in the influent water both before and 15 days after scraping (qPCR $p = 0.004$) (Fig. 2D).

3.2. Microbial community composition

The microbial communities of the influent and effluent water and sand were dominated by different taxa (Table S1). The families *Methylomonadaceae* (11.9 %), *Comamonadaceae* (5.9 %), *Gallionellaceae* (5.8 %) and *Methylopilaceae* (4.7 %) were only abundant in the influent, whereas an unclassified family within the order PLTA-13 (16.6 %), *Gemmataceae* (7.6 %), *Pirellulaceae* (4.8 %), A4b (2.5 %) and *Entotheonellaceae* (2.1 %) were mainly present in the sand samples. Finally, *Omnitrophaceae* (9.2 %), as well as unclassified families within the order *Rokubacteriales* (6.4 %) and the class *Thermodesulfovibrionia* (5.8 %) were only dominant in the water influent and, thus, did not reflect the microbial community of the sand.

3.2.1. Sand

The top 2 cm of the scraped filter before scraping (day 0) and the control filter had similar dominant taxa (Table S1). The PCoA plot of the beta-diversity analysis (Fig. 4) also indicated that these two filters had a similar community since both samples were almost identical on the first axis of the PCoA plot which explained 76 % of the data variance. After scraping, the sand microbial community composition of the scraped filter shifted to the left side of the plot already at day 8, indicating a notable impact of scraping on the community composition in the top layer. However, after scraping the community in the top 2 cm resembled the composition in the deeper layers (10–15 and 20–25 cm) in the filter before scraping (Fig. S4). This shift can be attributed to the fact that approximately 10 cm of sand is manually removed during the scraping process, making the 10 cm depth of the pre-scraped filter the new surface (0–2 cm) in the filter after scraping.

Scraping changed the relative abundance of some of the dominant taxa in the top layer of the SSF, with mainly an increase in an unclassified family within the order PLTA13, whereas *Gemmataceae* and A4b decreased. Despite these shifts, the main taxa like PLTA13, *Nitrospiraceae*, *Gemmataceae*, *Vicinamibacteriales*, *Pirellulaceae*, *Vicinamibacteriaceae*, *Nitrosomonadaceae*, *Nitrosopumilaceae*, A4b and *Hyphomicrobiaceae* remained prevalent both before and after scraping (Table 2 and Fig. 5). However, a substantial decrease in the overall

Table 2
A heatmap of the top 35 dominant taxa found in the sand from 0–2 cm depth of both scraped and control filters. The taxa sre shown at family level, if they are only classified at a higher taxonomic level (order, class, phylum), those are indicated. Darker red-colored cells signify higher relative abundance of taxa, whereas lighter red indicates lower abundance.

	RELATIVE ABUNDANCE							
	Scraped filter					Control filter		
	Day 0	Day 8	Day 15	Day 28	Day 52	Day 8	Day 28	Day 52
PLTA13--Order	4.9	17.1	19.5	19.6	24.7	4.4	6.4	6.9
Nitrospira	12.6	6.1	11.0	11.5	9.6	5.3	9.4	10.7
Gemmataceae--Family	12.0	6.8	5.9	6.1	2.4	11.5	10.2	10.2
Vicinamibacterales--Order	4.3	5.0	3.6	3.7	3.1	6.8	5.0	5.6
Vicinamibacteraceae--Family	2.7	3.6	2.2	2.6	3.2	5.3	4.0	5.2
A4b--Family	7.0	1.7	0.8	0.9	0.9	5.8	4.2	4.4
Pirellulaceae--Family	1.4	3.0	2.9	2.5	2.0	1.5	2.0	0.9
BD2-11_terrestrial_group--Class	1.5	1.5	1.9	2.2	2.0	1.0	2.3	2.0
TRA3-20--Family	1.8	2.5	1.8	2.0	3.0	1.5	0.8	0.9
Nitrosopumilaceae--Family	0.2	2.7	2.6	4.6	3.2	0.1	0.1	0.2
Blastocatellaceae--Family	2.0	0.8	0.5	0.7	1.2	1.6	1.6	4.0
Latescibacterota--Phylum	0.7	0.6	1.3	1.5	2.3	1.4	2.7	2.0
Subgroup_17--Order	1.1	1.6	1.7	1.8	2.6	0.8	1.3	1.5
RCP2-54--Phylum	2.3	2.3	1.4	1.7	1.5	1.9	0.7	0.6
SWB02	1.3	1.0	1.0	1.3	1.0	2.6	2.2	2.0
OM190--Class	1.6	0.7	1.7	2.0	2.0	0.7	2.0	1.3
MND1	0.9	1.1	1.4	1.7	2.6	0.5	1.6	2.1
RBG-13-54-9--Order	0.7	0.7	2.0	2.4	2.4	0.3	1.3	1.9
Comamonadaceae--Family	1.3	0.3	0.7	0.9	1.2	1.1	1.9	3.4
Gaiellales--Order	0.6	1.9	2.0	1.7	1.2	1.0	1.2	0.8
Pedomicrobium	1.4	0.7	0.7	0.6	0.9	2.6	1.7	1.8
Entotheonellaceae--Family	1.7	2.1	0.7	0.8	0.7	1.3	1.4	1.4
NB1-j--Phylum	1.5	1.6	1.8	1.6	1.3	0.4	0.3	0.2
Anaerolineaceae--Family	1.1	0.1	0.0	0.0	0.0	1.9	3.4	2.2
Subgroup_9--Order	1.1	2.1	1.8	1.2	1.0	0.4	0.4	0.1
MB-A2-108--Class	0.7	1.5	1.6	1.3	0.7	0.9	1.0	0.4
B1-7BS--Family	1.3	0.9	0.4	0.5	0.5	1.9	1.2	1.1
Gemmata	0.8	0.8	0.9	0.8	0.6	1.5	1.1	1.2
Pirellula	0.9	1.3	0.9	0.8	0.9	1.1	0.8	0.9
Pir4_lineage	0.7	1.1	1.1	0.9	0.9	0.9	0.9	0.8
mle1-7	0.6	0.9	1.3	1.3	1.8	0.2	0.6	0.6
S085--Order	0.5	0.4	0.7	0.4	0.6	1.1	2.1	1.5
Planctomycetales--Order	1.2	0.6	0.4	0.5	0.5	0.7	1.1	1.6
IS-44	0.7	0.6	0.9	0.7	1.2	0.6	0.8	1.2
Rhizobiales_Incertae_Sedis--Family	1.0	0.9	0.6	0.5	0.5	1.3	0.7	0.6

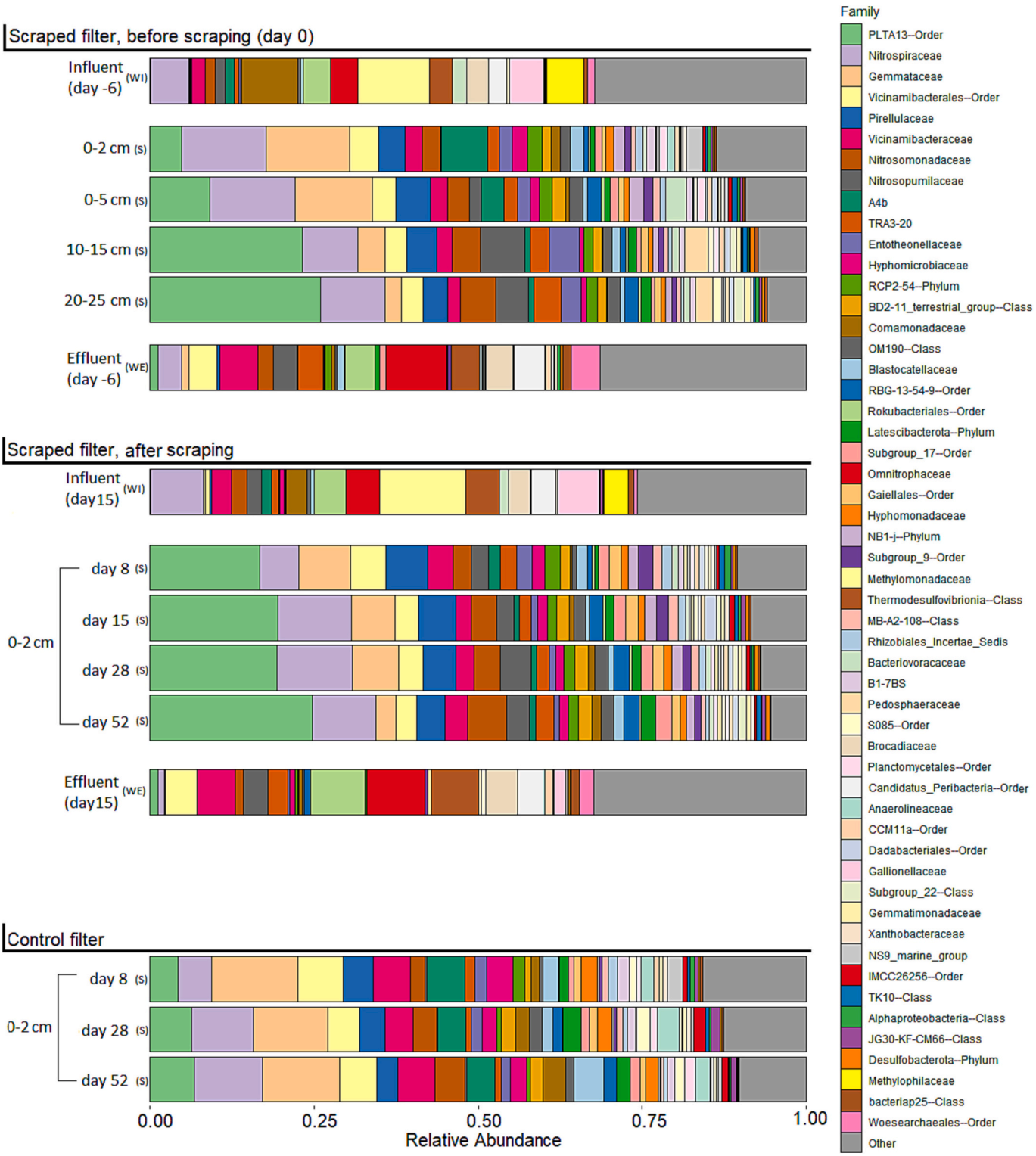

Fig. 5. Microbial community composition bar plot of sand in scraped and control filters at different depths (scraped filter) and at different time points. Relative abundance of the top 53 taxa at family level is shown as the average of two duplicate biological replicates. The taxa are shown at family level, if they that are only classified at a higher taxonomic levels (order, class, phylum), those classifications are indicated.

biomass load occurred in the top layer as shown in Fig. 2B, demonstrating that although the relative abundance for most taxa remained similar, the absolute abundance of these taxa decreased due to scraping.

3.2.2. Water

The microbial community composition of the effluent water before (day −6) and 15 days after scraping was comparable, and both were distinctly different from the community in the influent water (Figs. 5 and 6). This observation was further supported by the results of the PERMANOVA test, indicating a significant difference between sampling points (influent and effluent) ($p = 0.031$). Additionally, there was no significant difference in microbial community composition when

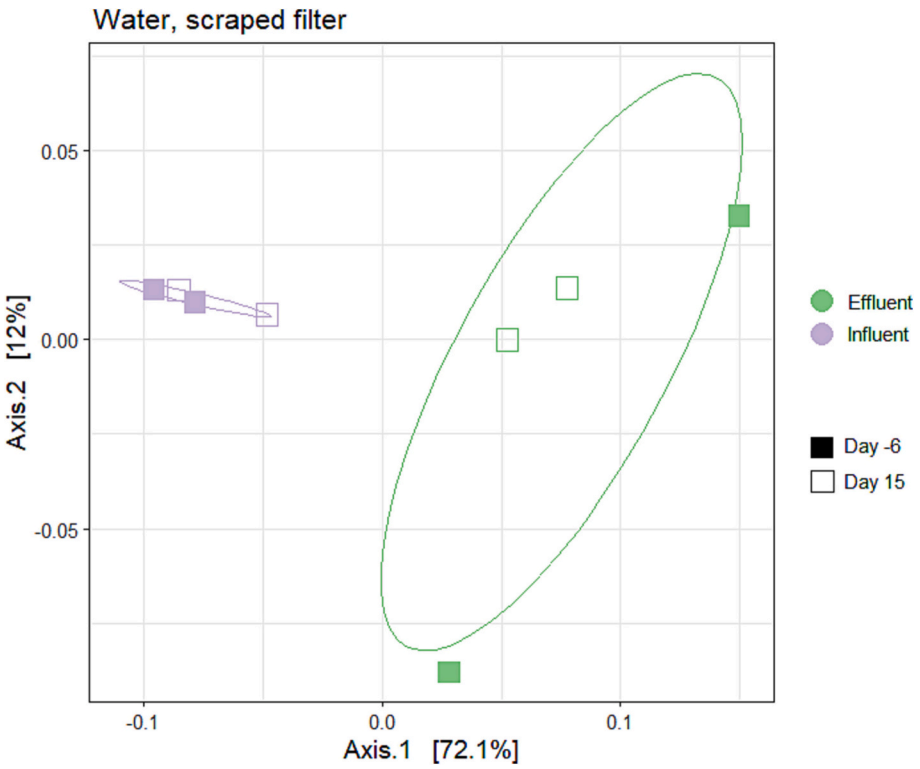

Fig. 6. PCoA plot showing the Beta Diversity (Weighted UniFrac) analysis of water samples from the scraped filter before (day −6) and 15 days after scraping.

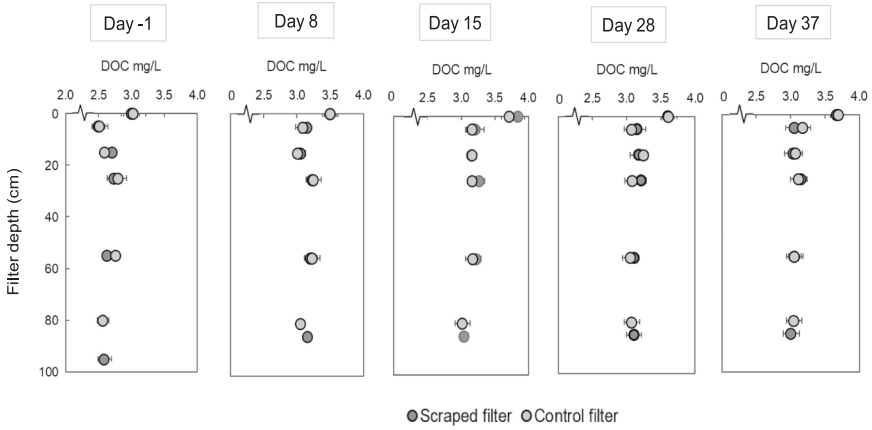

Fig. 7. Depth profiles of DOC in scraped and control filters during filter operation. Measurements were carried out in triplicates; error bars represent standard deviation.

considering the sampling day ($p = 0.655$).

3.3. Concentrations of DOC, NH_4^+ and NO_3^-

The influent DOC concentration ranged from 2.4 to 3.7 mg/L during the monitoring period of 37 days (Fig. 7). On day −1, both filters reduced the DOC concentration by 0.6–0.7 mg/L, with most of the removal in the top 5 cm. After scraping, the depth profiles of DOC remained consistent with the concentrations measured before scraping or in the control SSF. Thus, no DOC release in the top layers was observed due to scraping, which contrasts with the ICC_w and $cATP_w$ data. A slight increase was noted in the middle layers, also seen in the control filter until day 28, suggesting the release was independent of scraping. However, this released DOC fraction was subsequently removed in the deeper layers. These observations suggest that DOC release in the deeper layers might be important to understand the overall DOC removal mechanisms.

NH_4^+ concentration in the influent was low and ranged from 5.8 to 8.1 μg N/L, while NO_3^- was between 1.41 and 1.61 mg N/L. The NH_4^+ concentration during the sampling period was close to the detection limit of 5 μg/L. NH_4^+ decreased in the first 55 cm and then stabilized. NO_3^- significantly increased in the deeper layers ($p = 0.0005$) (Fig. 8). Both NH_4^+ and NO_3^- concentrations were not significantly different ($p = 0.09$) between the scraped and control SSF. The depth profiles of NH_4^+ and NO_3^-, thus, remained stable after scraping, indicating that NH_4^+ removal was not controlled by the top layer biofilms alone.

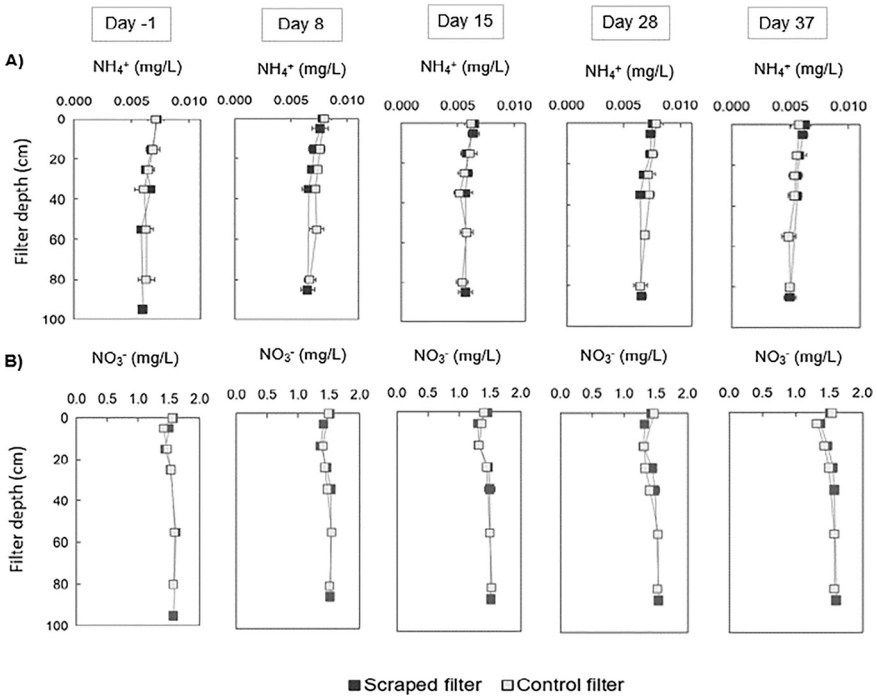

Fig. 8. Depth profiles of NH_4^+ (A) and NO_3^- (B) in scraped and control filters during filter operation. Measurements were carried out in triplicates; error bars represent standard deviation.

4. Discussion

4.1. Filter recovery after scraping

This research examined operating scraped and unscraped mature full-scale SSFs along the filter depth to examine the recovery processes after scraping. $cATP_w$, $HNA\text{-}ICC_w$ and $LNA\text{-}ICC_w$ in water from the top layers increased immediately after scraping. This deterioration of cATPw and ICCw could be attributed to bacterial sloughing of the filter biofilm [26] and/or reduced retention of microbial biomass in the water from top layers after the *Schmutzdecke* removal. Straining in the *Schmutzdecke* has been observed to be a key retention mechanism for bacteria [39–41]. However, biomass released from the top layers after scraping was retained in the deeper layers. This highlights the role of physical-chemical and biological processes in the sand bed and the adaptability of mature filters to *Schmutzdecke* loss. In contrast, newer filters have been shown to be strongly impacted by scraping, resulting in poor removal of total organic carbon and bacterial indicators [2,9,10,39]. This contrast may be due to differences in maturity of microbial communities across filters [42]. In newer filters without established biofilms in the sand bed, effluent quality is more dependent on the *Schmutzdecke* layer [9,10,39]. Therefore, depth profiles must be monitored to assess disruption and/or recovery of microbial biomass after scraping.

In DWTPs where SSF is the final treatment step [3], understanding the impact of scraping on disinfection is vital to ensure microbial safety of produced drinking water, necessitating the analysis of fecal indicators and pathogens in the effluent. Pathogen removal was not explored in this research, as these organisms were not detected in the influent. Previously, deeper layers of mature SSFs have shown substantial bacteria and virus removal capacity as the *Schmutzdecke* [41]. Chan et al. reported no breakthrough of coliform and *E. coli* in the effluent after scraping of mature full-scale SSFs [9]. However, future research should examine scraping effects on fecal virus, bacteria and protozoa removal and explore how pathogen removal processes recover in new and mature full-scale SSFs.

Scraping reduced biomass in the top sand layers, as previously reported by De Souza et al. [11]. Yet, biomass redeveloped after scraping as expected due to high nutrient levels in the influent, compared to biomass concentration. The altered microbial community composition resembled that of the deeper layers. This change is not attributed to a shift in the community composition, but to scraping of top 10 cm of the sand bed, which exposed deeper layers to the surface. Despite a shift in the relative abundances of various microbial groups, certain dominant taxa such as PLTA13, *Nitrospiraceae*, *Gemmataceae*, *Vicinamibacteriales*, *Pirellulaceae*, *Vicinamibacteriaceae*, *Nitrosomonadaceae*, *Nitrosopumilaceae* and A4B remained prevalent in the top layers even after scraping. A previous lab-scale investigation found depth stratification of bacterial community after scraping [11]. In the present study with mature full-scale SSFs, the dominant taxa were not confined to the *Schmutzdecke*, but extended beyond the top 10 to 15 cm. Although microbial biomass in the top layer was reduced after scraping, the relative abundance of the dominant groups remained unchanged. Therefore, the integration of relative and absolute abundances of microbial community using 16S rRNA gene amplicon sequencing, qPCR and ATP methods offers a comprehensive view of the dynamics of microbial abundance and diversity within the SSFs.

Despite disturbances from scraping, the microbial community composition in filter effluent before and after scraping was similar, indicating the system's resilience to short-term disruptions. Moreover, both before and after scraping, the effluent microbial community differed significantly from the influent ($p = 0.031$) and its biomass content (measured with qPCR) was still lower than in the influent, proving the capability of SSFs to retain bacterial biomass within 15 days after scraping. These findings highlight the resilience and robustness of mature SSF microbial communities and the contribution of the deepest layers of the sand bed in maintaining the treatment efficiency after the removal of the top layer.

4.2. DOC and NH_4^+ removal processes

The SSFs consistently reduced DOC by 0.5 mg/L, with scraping showing no adverse effect on DOC levels at varying filter depths. However, the decrease in DOC was not solely due to the easily

biodegradable organic carbon fractions. The influent and effluent data (Table 1) show that the influent AOC concentration of 5.4 μg C/L, already within the guideline value of 10 μg C/L for biostable water [43] decreased to 3.6 μg C/L in the effluent. This suggests that the removed DOC contained complex, recalcitrant organic carbon fractions, such as polysaccharides and humic substances, similar to previous findings [19,44]. Since fractions like humics are difficult to degrade in SSFs, physical-chemical processes alongside microbial processes might have contributed to DOC removal [2]. DOC release in the middle layers has been reported previously in biological filtration systems, linked to biofilm proliferation and breakdown of particulate organic carbon into DOC [45,46]. Furthermore, the concentration of released DOC may be reduced in the deeper layers by a combination of physical-chemical and microbial processes.

Heterotrophs play a crucial role in the carbon cycle by metabolizing BDOC. Various microbial groups including those with cultivated heterotrophic species such as *Gemmataceae*, and *Vicinamibacteraceae* [47,48] dominated the microbial community across all filter depths (Fig. 5). This might indicate the potential ability of the SSF microbial community to degrade BDOC and produce biologically stable drinking water throughout the filter depth. However, specific microorganisms within these dominant groups responsible for BDOC degradation are difficult to pinpoint due to the unclassified nature of many genera. Identifying these microbes is essential for a clearer understanding of the carbon cycle and for enhancing water treatment techniques. Yet, it's important to note that 16S rRNA gene amplicon sequencing, while useful, has its limitations in providing comprehensive functional insights due to its inability to fully capture microbial functionality. More advanced techniques such as metagenomics, metatranscriptomics and proteomics offer more detailed insight into the functional potential of the microbial community and could be used to determine microbial roles in decomposing organic substances. Furthermore, innovative approaches like bioorthogonal non-canonical amino acid tagging combined with fluorescence-activated cell sorting (BONCAT-FACS) [49,50] and cultivation methods might help to identify microbes responsible for BDOC degradation. However, mimicking low BDOC levels in SSF influent poses significant analytical challenges.

NH_4^+ removal occurred over the filter depth, indicating the occurrence of nitrification. *Nitrospiraceae* (dominated by the genus *Nitrospira*), *Nitrosomonadaceae* and *Nitrosopumilaceae* families, capable of oxidizing ammonia and/or nitrite were observed in the filter sand [51,52]. The dominance of *Nitrospira* indicates direct NH_4^+ oxidation to NO_3^- as members of this genus have been shown for their capacity to perform complete oxidation of ammonia, also referred to as comammox metabolism [22,51,52]. *Nitrospiraceae*, *Nitrosomonadaceae* and *Nitrosopumilaceae* were not only present in the filter but also in the influent which might be a carryover from the preceding rapid sand filtration step where NH_4^+ is actively removed and continued to persist throughout the filter bed. *Nitrosopumilaceae* are known to thrive at lower ammonia concentrations compared to *Nitrospiraceae* and *Nitrosomonadacae* [53]. Therefore, the increased relative abundance of *Nitrosopumilaceae* in deeper layers suggests NH_4^+ depletion from its removal in the top layers. The diversity of microbial communities enhances NH_4^+ removal, adapting to varying NH_4^+ concentrations and environmental conditions. Therefore, it is important to preserve microbial diversity in the filter to improve water treatment effectiveness.

4.3. Implications for practice

SSFs in this study received pre-treated influent from managed aquifer recharge (infiltration of pretreated river water in the dunes and subsequent abstraction) and rapid sand filtration. This has greatly reduced microbial and organic load and thereby the extent of clogging in SSFs. Since deeper layers of full-scale SSF were unaltered during scraping for over 67 years, microbial communities and purification processes remained resilient in the sand bed. Thus, deeper layer biofilms should be retained in the filter by avoiding repetitive scraping. Backwashing may be used as an alternative to traditional scraping to preserve biomass within the filter for quick recovery of full filter function.

Future research could examine removal of pathogens and biological stability indicators such as microbial growth potential and biofouling potential. This evaluation is important to clarify if mature SSFs, especially under low-loading conditions, require a ripening period or not. Whereas, in young filters without optimally performing biofilms in the deep sand bed, a ripening period might be necessary to recover filter performance. The ripening of these young filters may be accelerated by biostimulation with nutrients, inoculation with specific microbial communities or filter media from mature SSFs. It is essential to note that the hypotheses outlined here are starting points that require further experimental validation. They provide a basis for future research to rigorously test and confirm these initial observations.

This research showed that recovery of microbial activity and ecology after scraping can be effectively monitored using rapid ATP and FCM, and 16S rRNA gene sequencing on influent, sand and effluent samples. Further, relying solely on effluent quality analyses is not sufficient to understand filter status, as deeper layers balance scraping effect. Therefore, depth profiles of previously mentioned microbial biomass parameters could be monitored to assess recovery and optimize SSF maintenance, thereby reducing costs and water loss.

5. Conclusions

This study compared the performance of scraped and unscraped mature full-scale SSFs to evaluate the recovery of microbial biomass and communities, and the removal of DOC and NH_4^+ after scraping. The main findings were:

- Scraping reduced microbial biomass on filter sand but did not alter the dominant prokaryotic taxa.
- ATP and flow cytometry analysis revealed temporary disruption in top layers after scraping when monitored over the height in mature SSFs.
- Stable effluent concentrations of DOC, NH_4^+, $cATP_w$ and ICC_w and consistent microbial community composition throughout ripening showed that deeper layer biofilms offset any scraping effect.
- Further research on the effects of scraping on fecal pathogens removal and biological stability parameters (e.g., regrowth potential) in mature SSFs is recommended to assess the need for filter ripening.

CRediT authorship contribution statement

Shreya Ajith Trikannad: Conceptualization, Data curation, Formal analysis, Investigation, Methodology, Software, Validation, Visualization, Writing – original draft. **Valentina Attiani:** Conceptualization, Data curation, Formal analysis, Investigation, Methodology, Software, Visualization, Writing – original draft. **Paul W.J.J. van der Wielen:** Supervision, Visualization, Writing – review & editing. **Hauke Smidt:** Supervision, Visualization, Writing – review & editing. **Jan Peter van der Hoek:** Conceptualization, Funding acquisition, Project administration, Supervision, Visualization, Writing – review & editing. **Doris van Halem:** Conceptualization, Supervision, Visualization, Writing – review & editing.

Declaration of competing interest

The authors declare that they have no known competing financial interests or personal relationships that could have appeared to influence the work reported in this paper.

Data availability

Data will be made available on request.

Acknowledgements

This study was performed within NWO-Dunea-Vitens partnership programme. The programme is funded by NWO, the national research council of the Netherlands (Project No. 17831). The authors acknowledge Thanisha Kannan for supporting the experimental work. We are grateful to Brent Pieterse, Clemy van der Steen-de Kok and Dunea Duin & Water for their support and collaboration during the visits to the drinking water plants. We would like to acknowledge the staff from TU Delft Waterlab, especially Armand Middeldorp and Jasper Krijn for their support in the laboratory.

Appendix A. Supplementary data

Supplementary data to this article can be found online at https://doi.org/10.1016/j.jwpe.2024.105101.

References

[1] E.I. Prest, F. Hammes, S. Kötzsch, M.C.M. Van Loosdrecht, J.S. Vrouwenvelder, A systematic approach for the assessment of bacterial growth-controlling factors linked to biological stability of drinking water in distribution systems, Water Sci. Technol. Water Supply 16 (4) (2016) 865–880.
[2] S.J. Haig, G. Collins, R.L. Davies, C.C. Dorea, C. Quince, Biological aspects of slow sand filtration: past, present and future, Water Sci. Technol. Water Supply 11 (4) (2011) 468–472.
[3] D. van der Kooij, H.R. Veenendaal, E.J. van der Mark, M. Dignum, Assessment of the microbial growth potential of slow sand filtrate with the biomass production potential test in comparison with the assimilable organic carbon method, Water Res. 125 (2017) 270–279.
[4] L. Huisman, W.E. Wood, Slow Sand Filtration, World Health Organization, 1974.
[5] X. Bai, I.J. Dinkla, G. Muyzer, Microbial ecology of biofiltration used for producing safe drinking water, Appl. Microbiol. Biotechnol. 106 (13–16) (2022) 4813–4829.
[6] S.J. Haig, C. Quince, R.L. Davies, C.C. Dorea, G. Collins, The relationship between microbial community evenness and function in slow sand filters, MBio 6 (5) (2015) e00729-15.
[7] S. Oh, F. Hammes, W.T. Liu, Metagenomic characterization of biofilter microbial communities in a full-scale drinking water treatment plant, Water Res. 128 (2018) 278–285.
[8] G.E. Symons, Water treatment through the ages, J. Am. Water Works Ass. 98 (3) (2006) 87–98.
[9] S. Chan, K. Pullerits, J. Riechelmann, K.M. Persson, P. Rådström, C.J. Paul, Monitoring biofilm function in new and matured full-scale slow sand filters using flow cytometric histogram image comparison (CHIC), Water Res. 138 (2018) 27–36.
[10] M. Robin Collins, M. Unger, Assessing Escherichia coli removal in the *Schmutzdecke*, J. Am. Water Works Assoc. 100 (12) (2008) 60–73.
[11] F.H. De Souza, P.B. Roecker, D.D. Silveira, M.L. Sens, L.C. Campos, Influence of slow sand filter cleaning process type on filter media biomass: backwashing versus scraping, Water Res. 189 (2021) 116581.
[12] M.J. Brandt, K.M. Johnson, A.J. Elphinston, D.D. Ratnayaka, Specialized and advanced water treatment processes, Twort's Water Supply (2017) 407–473.
[13] R. Schurer, W.A.M. Hijnen, A. van der Wal, The significance of the biomass subfraction of high-MW organic carbon for the microbial growth and maintenance potential of disinfectant-free drinking water produced from surface water, Water Res. 209 (2022) 11789.
[14] P.W. van der Wielen, A. Brouwer-Hanzens, R. Italiaander, W.A. Hijnen, Initiating guidance values for novel biological stability parameters in drinking water to control regrowth in the distribution system, Sci. Total Environ. 871 (2023) 161930.
[15] J.W. Park, H.C. Kim, A.S. Meyer, S. Kim, S.K. Maeng, Influences of NOM composition and bacteriological characteristics on biological stability in a full-scale drinking water treatment plant, Chemosphere 160 (2016) 189–198.
[16] F. Hammes, C. Berger, O. Köster, T. Egli, Assessing biological stability of drinking water without disinfectant residuals in a full-scale water supply system, J. Water Supply Res. Technol. AQUA 59 (1) (2010) 31–40.
[17] U. Hübner, U. Miehe, M. Jekel, Optimized removal of dissolved organic carbon and trace organic contaminants during combined ozonation and artificial groundwater recharge, Water Res. 46 (18) (2012) 6059–6068.
[18] S.J. Haig, Characterising the Functional Ecology of Slow Sand Filters Through Environmental Genomics (Doctoral dissertation), University of Glasgow, 2014.
[19] K. Lautenschlager, C. Hwang, F. Ling, W.T. Liu, N. Boon, O. Köster, F. Hammes, Abundance and composition of indigenous bacterial communities in a multi-step biofiltration-based drinking water treatment plant, Water Res. 62 (2014) 40–52.
[20] S. Velten, M. Boller, O. Köster, J. Helbing, H.U. Weilenmann, F. Hammes, Development of biomass in a drinking water granular active carbon (GAC) filter, Water Res. 45 (19) (2011) 6347–6354.
[21] K. Tatari, B.F. Smets, H.J. Albrechtsen, A novel bench-scale column assay to investigate site-specific nitrification biokinetics in biological rapid sand filters, Water Res. 47 (16) (2013) 6380–6387.
[22] M.A. Van Kessel, D.R. Speth, M. Albertsen, P.H. Nielsen, H.J. Op den Camp, B. Kartal, S. Lücker, Complete nitrification by a single microorganism, Nature 528 (7583) (2015) 555–559.
[23] Y. Adomat, G.H. Orzechowski, M. Pelger, R. Haas, R. Bartak, Z.A. Nagy-Kovacs, T. Grischek, New methods for microbiological monitoring at riverbank filtration sites, Water 12 (2) (2020) 584.
[24] G.A. de Vera, E.C. Wert, Using discrete and online ATP measurements to evaluate regrowth potential following ozonation and (non) biological drinking water treatment, Water Res. 154 (2019) 377–386.
[25] E.I. Prest, F. Hammes, S. Kötzsch, M.C. van Loosdrecht, J.S. Vrouwenvelder, Monitoring microbiological changes in drinking water systems using a fast and reproducible flow cytometric method, Water Res. 47 (19) (2013) 7131–7142.
[26] M. Sousi, G. Liu, S.G. Salinas-Rodriguez, L. Chen, J. Dusseldorp, P. Wessels, W. van der Meer, Multi-parametric assessment of biological stability of drinking water produced from groundwater: reverse osmosis vs. conventional treatment, Water Res. 186 (2020) 116317.
[27] Investigation of backwash strategy on headloss development and particle release in drinking water biofiltration.
[28] A. Apprill, S. McNally, R. Parsons, L. Weber, Minor revision to V4 region SSU rRNA 806R gene primer greatly increases detection of SAR11 bacterioplankton, Aqua, Microb. Ecol. 75 (2) (2015) 129–137.
[29] A.E. Parada, D.M. Needham, J.A. Fuhrman, Every base matters: assessing small subunit rRNA primers for marine microbiomes with mock communities, time series and global field samples, Environ. Microbiol. 18 (5) (2016) 1403–1414.
[30] W. Poncheewin, G.D. Hermes, Van Dam, J.J. Koehorst, H. Smidt, P.J. Schaap, NG-Tax 2.0: a semantic framework for high-throughput amplicon analysis, Front. in Gen. 10 (2020) 1366.
[31] J. Ramiro-Garcia, G.D. Hermes, C. Giatsis, D. Sipkema, E.G. Zoetendal, P.J. Schaap, H. Smidt, NG-Tax, a highly accurate and validated pipeline for analysis of 16S rRNA amplicons from complex biomes F1000Res., (2016) 5.
[32] C. Quast, E. Pruesse, P. Yilmaz, J. Gerken, T. Schweer, P. Yarza, J. Peplies, F. O. Glöckner, The SILVA ribosomal RNA gene database project: improved data processing and web-based tools, Nucleic Acids Res. 41 (D1) (2013) D590–D596.
[33] P.J. McMurdie, S. Holmes, phyloseq: an R package for reproducible interactive analysis and graphics of microbiome census data, PloS one 8 (4) (2013) e61217.
[34] D.J. Barnett, I.C. Arts, J. Penders, microViz: an R package for microbiome data visualization and statistics, J. of Open Sour. Softw. 6 (63) (2021) 3201, https://doi.org/10.21105/joss.03201.
[35] C. Ahlmann-Eltze, I. Patil, ggsignif: R Package for Displaying Significance Brackets for'ggplot2, PsyArxiv (2021), https://doi.org/10.31234/osf.io/7awm6.
[36] M. McLaren, speedyseq: Faster implementations of phyloseq functions. https://github.com/mikemc/speedyseq https://github.com/mikemc/speedyseq.
[37] E. Neuwirth, ColorBrewer: ColorBrewer Palettes, R package version 1.1-3, 2022. https://CRAN.R-project.org/package=RColorBrewer.
[38] J. Oksanen, G. Simpson, F. Blanchet, R. Kindt, P. Legendre, P. Minchin, R. O'Hara, P. Solymos, M. Stevens, E. Szoecs, H. Wagner, M. Barbour, M. Bedward, B. Bolker, D. Borcard, G. Carvalho, M. Chirico, M. De Caceres, S. Durand, H. Evangelista, R. FitzJohn, M. Friendly, B. Furneaux, G. Hannigan, M. Hill, L. Lahti, D. McGlinn, M. Ouellette, E. Ribeiro Cunha, T. Smith, A. Stier, C. Ter Braak, J. Weedon, vegan: Community Ecology Package, R package version 2.6-4, 2022.
[39] W.A. Hijnen, J.F. Schijven, P. Bonne, A. Visser, G.J. Medema, Elimination of viruses, bacteria and protozoan oocysts by slow sand filtration, Water Sci. Technol. 50 (1) (2004) 147–154.
[40] W.A. Hijnen, Y.J. Dullemont, J.F. Schijven, A.J. Hanzens-Brouwer, M. Rosielle, G. Medema, Removal and fate of Cryptosporidium parvum, Clostridium perfringens and small-sized centric diatoms (Stephanodiscus hantzschii) in slow sand filters, Water Res. 41 (10) (2007) 2151–2162.
[41] S.A. Trikannad, D. van Halem, J.W. Foppen, J.P. van der Hoek, The contribution of deeper layers in slow sand filters to pathogens removal, Water Res. 237 (2023) 119994.
[42] L. Abkar, H.S. Moghaddam, S.J. Fowler, Microbial ecology of drinking water from source to tap, Sci. Total Environ. 908 (2024) 168077.
[43] W.A. Hijnen, D. Van Der Kooij, AOC removal and accumulation of bacteria in experimental sand filters, Revue des sciences de l'eau 5 (1992) 17–32.
[44] L.C. Campos, M.F.J. Su, N.J.D. Graham, S.R. Smith, Biomass development in slow sand filters, Water Res. 36 (18) (2002) 4543–4551.
[45] E. Bar-Zeev, N. Belkin, B. Liberman, T. Berman, I. Berman-Frank, Rapid sand filtration pretreatment for SWRO: microbial maturation dynamics and filtration efficiency of organic matter, Desalination 286 (2012) 120–130.
[46] N. Perujo, A.M. Romaní, X. Sánchez-Vila, Bilayer infiltration system combines benefits from both coarse and fine sands promoting nutrient accumulation in sediments and increasing removal rates, Environ. Sci. Technol. 52 (10) (2018) 5734–5743.
[47] I.S. Kulichevskaya, A.A. Ivanova, O.I. Baulina, W.I.C. Rijpstra, J.S. Sinninghe Damsté, S.N. Dedysh, Fimbriiglobus ruber gen. nov., sp. nov., a Gemmata-like planctomycete from Sphagnum peat bog and the proposal of Gemmataceae fam. nov, Int. J. Syst. Evol. Microbiol. 67 (2) (2017) 218–224.
[48] K.J. Huber, J. Overmann, Vicinamibacteraceae fam. nov., the first described family within the subdivision 6 Acidobacteria, Int. J. Syst. Evol. Microbiol. 68 (7) (2018) 2331–2334.

[49] E. Couradeau, J. Sasse, D. Goudeau, N. Nath, T.C. Hazen, B.P. Bowen, T. R. Northen, Probing the active fraction of soil microbiomes using BONCAT-FACS, Nat. Commun. 10 (1) (2019) 2770.
[50] R. Hatzenpichler, S.A. Connon, D. Goudeau, R.R. Malmstrom, T. Woyke, V. J. Orphan, Visualizing in situ translational activity for identifying and sorting slow-growing archaeal–bacterial consortia, Proc. Natl. Acad. Sci. 113 (28) (2016) E4069–E4078.
[51] S. Haukelidsaeter, A.S. Boersma, L. Kirwan, A. Corbetta, I.D. Gorres, W.K. Lenstra, C.P. Slomp, Influence of filter age on Fe, Mn and NH4+ removal in dual media rapid sand filters used for drinking water production, Water Res. 242 (2023) 120184.
[52] H. Daims, E.V. Lebedeva, P. Pjevac, P. Han, C. Herbold, M. Albertsen, M. Wagner, Complete nitrification by Nitrospira bacteria, Nature 528 (7583) (2015) 504–509.
[53] M.Y. Jung, C.J. Sedlacek, K.D. Kits, A.J. Mueller, S.K. Rhee, L. Hink, M. Wagner, Ammonia-oxidizing archaea possess a wide range of cellular ammonia affinities, ISME J. 16 (1) (2022) 272–283.